Agro-Industrial Kiwifruit Waste as a Renewable Feedstock for Hydrogen Production - A Study of Feedstock Viability

Enola Brecht and Peter Kovalsky *

Posted Date: 26 February 2026

doi: 10.20944/preprints202602.1296.v1

Keywords: agro-industrial kiwifruit & apple waste; anaerobic digestion; biomethane; biomethane potential; steam methane reforming; hydrogen

 doi:10.20944/preprints202602.1296.v1

Article

Agro-Industrial Kiwifruit Waste as a Renewable Feedstock for Hydrogen Production - A Study of Feedstock Viability

Enola Brecht [1,2] and Peter Kovalsky [2,*]

[1] Department of Biotechnology, University of Applied Sciences Mannheim, Paul-Wittsack-Straße 10, 68163 Mannheim, Germany

[2] School of Engineering, University of Waikato, Private Bag 3105, Hamilton 3240, New Zealand

* Correspondence: peter.kovalsky@waikato.ac.nz

Abstract

NewZealand's kiwifruit are major contributors to the nation's horticultural exports. However, it produces large volumes of organic waste. This study investigates the potential of agro-industrial kiwifruit waste as feedstock for hydrogen generation via anaerobic digestion and steam reforming. Two feedstock mixtures were examined, a 50:50 blend of kiwifruit and apple, and a second mixture supplemented with potato to mitigate acidification. Cow manure was used as a cost-effective inoculum for anaerobic digestion. Physicochemical analysis confirmed that both feedstock mixtures were generally suitable. Biomethane potential tests were conducted. Methane yields ranged from 0 to 20 mLCH4/gVSadded, with the best result 45 mLCH4/gVSadded achieved by mixture 2 at ISR 4, corresponding to a 46.5% carbon conversion. From a total waste amount of 476 tonnes, a theoretical yield of 8,000 m3 of biomethane could be produced. Steam methane reforming simulations confirmed the viability of biogas as an alternative to natural gas, although its higher sulfur content may necessitate more frequent catalyst replacement. With a 46% methane conversion efficiency, an estimated 7,600 m3 of hydrogen could be produced. This study offers a practical foundation for converting kiwifruit and apple waste into renewable hydrogen, supporting New Zealand's decarbonization and circular economy objectives.

Keywords: agro-industrial kiwifruit & apple waste; anaerobic digestion; biomethane; biomethane potential; steam methane reforming; hydrogen

1. Introduction

New Zealand is prominent for its kiwifruit and apple industries, which play a significant role in the nation's horticultural exports. The kiwifruit sector, New Zealand's largest horticulture, produces approximately 184 million trays annually, exporting to over 60 countries, which generated $2.9 billion in 2022. Over 80% from the 13,610 hectares of the crop are grown in the Bay of Plenty region [1,2]. Similarly, New Zealand leads in apple production with a yield of 61 tons per hectare, which exceeds the global average of 23.4, and exports 65% of its harvest [3]. However, both industries face the challenge of generating large amounts of organic waste during thinning and harvest. Thinning is performed multiple times during the growing season to optimize fruit quality by removing low-value or excess fruits, which is a critical practice for achieving export standards [2,4,5]. Despite its high organic content, most fruit waste from the kiwifruit and apple industries is either composted or sent to landfills, contributing to greenhouse gas emissions. In 2022, around three-quarters of waste sector emissions in New Zealand originated from landfill sites [6]. As efforts to cut greenhouse gas emissions and promote a circular economy intensify, repurposing this waste into hydrogen through digestion presents a promising solution.

 doi:10.20944/preprints202602.1296.v1

This article explores the potential of using this organic waste as feedstock for hydrogen production in New Zealand as a renewable alternative to fossil-based hydrogen. Given the nature of the feedstock, the chosen process must capitalize on its high organic content and water-rich composition, necessitating a biotechnological approach. Furthermore, this process is designed to be synergistic with existing infrastructure and technology to minimize investment costs.

Hydrogen is a non-toxic, clean energy carrier with significant potential to achieve carbon neutrality and support New Zealand's transition to net-zero emissions by 2050 [7,8]. It is compatible with renewable energy sources, can be stored long-term, transported via pipelines, and serves as a key chemical feedstock in industries such as petrochemicals, food processing, and metallurgy [7,9]. Currently, hydrogen production in New Zealand relies primarily on steam methane reforming (SMR) from natural gas, generating 10–19 tons of CO_2 per ton of hydrogen produced [10,11]. However, with impending natural gas shortages and the country's carbon neutrality commitments, facilities like Methanex, Evonik, and Agri-Ballance must transition to low-carbon hydrogen production in the near future [8,12]. This shift is also evident in the transport sector, where hydrogen adoption remains in its early stages, but fueling stations are being established across the country [13].

A comprehensive literature review identified various hydrogen production pathways from apple and kiwifruit waste, including microbial electrohydrogenesis, light and dark fermentation, cell-free synthetic biotransformation, ethanol fermentation with reforming, and anaerobic digestion combined with steam methane reforming.

Microbial electrohydrogenesis utilizes exoelectrogenic bacteria in microbial electrolysis cells to convert organic matter into hydrogen. While promising for organic waste utilization and mild operating conditions, its currently low efficiency, high costs, and need for specific electrode materials limit its viability [14–17].

Light Fermentation employs photosynthetic bacteria or microalgae to generate hydrogen from solar energy. However, its low light conversion efficiency due to saturation effects and the requirement for large-scale photobioreactors make it impractical for commercial applications [18–20].

Dark fermentation is an anaerobic process in which microorganisms break down carbohydrates to produce hydrogen. Species such as *Enterobacter*, *Bacillus*, and *Clostridium* utilize hydrogenase enzymes to re-oxidize reduced cofactors like ferredoxin and NAD. Among them, *Clostridium* achieves the highest yield (2.36 mol H_2 per mol glucose), though this remains relatively low [21]. By-product accumulation and the need for specific microbial cultures further hinder its scalability in New Zealand [18,20].

Cell-free synthetic pathway biotransformation (SyPaB) employs purified enzymes and coenzymes for hydrogen production, offering higher reaction rates compared to cell-based processes [22]. This method achieves a favorable energy efficiency ratio of 1.22 (hydrogen output to carbohydrate input) by absorbing ambient waste heat [23]. However, its reliance on costly enzyme production, purification, and stabilization limits economic feasibility.

Ethanol Fermentation with Reforming combines bioethanol production from biomass with ethanol steam reforming to generate hydrogen. Due to its low toxicity, low volatility, ease of handling, and established storage and transport infrastructure, is ethanol an attractive chemical compound for sustainable hydrogen production [24]. While scalable and compatible with renewable feedstocks [25–27], this method was not chosen.

While each method offers unique advantages, it also presents critical limitations that currently hinder large-scale implementation in New Zealand. By contrast, anaerobic digestion followed by steam methane reforming presents a viable pathway due to its ability to convert high-moisture organic waste into biogas efficiently, while leveraging already existing SMR infrastructure for hydrogen production.

Anaerobic digestion is a microbial process consisting of four stages: hydrolysis, acidogenesis, acetogenesis, and methanogenesis. During this process, organic matter is broken down, producing methane, carbon dioxide, and trace amounts of ammonia and hydrogen sulfide [28,29]. In the hydrolysis phase, enzymes degrade complex polymers into simpler compounds; however,

 doi:10.20944/preprints202602.1296.v1

lignocellulosic materials often require pretreatment to enhance biodegradability [30–32]. Acidogenesis then converts these monomers into volatile fatty acids (VFAs). Excessive accumulation can lead to acidification, disrupting the process [30,33]. During acetogenesis, VFAs are further converted into acetate, with hydrogenotrophic methanogens consuming hydrogen to maintain favorable conditions for acetogenic microorganisms [30,34]. Methanogenesis completes the process, producing methane under anaerobic conditions. Approximately two-thirds of methane are derived from the methyl group of acetate (acetoclastic methanogenesis), while about one-third originates from hydrogen via the carbon dioxide reduction pathway (hydrogenotrophic methanogenesis). Additionally, certain methanogens can utilize alternative substrates such as methanol and formate [30,35]. However, methanogens are slow-growing and highly sensitive to oxygen, making them a key limiting factor in AD efficiency [30,36].

Several factors influence AD performance, including temperature, pH, mixing, organic loading rate, C/N ratio, and hydraulic retention time. Maintaining optimal conditions is critical to prevent acidification, the accumulation of inhibitory compounds, and process imbalances that could reduce methane production efficiency [28,30,37–40]. AD systems can be classified as wet or dry digesters. Wet digesters, which are more commonly used, process feedstocks with a solids content below 15%, typically in slurry form, making them suitable for liquid-rich materials. In contrast, dry digesters handle feedstocks with over 15% solids, often in a stackable form. Agricultural fruit waste spans both categories; lignocellulosic early-thinning byproducts generally require pretreatment, whereas ripened fruit are better suited for wet digestion [41].

Before use in SMR, biogas must be purified to biomethane to prevent catalyst poisoning and system corrosion. Hydrogen sulfide (H_2S) is the primary contaminant, posing a significant sulfur poisoning risk [42]. Common H_2S removal methods include water and alkaline scrubbing, activated carbon filtration, and biological approaches such as *Thiobacillus*-based biofiltration, which is cost-effective and highly efficient [43].

In conventional steam methane reforming, methane reacts endothermically with steam to produce hydrogen and carbon monoxide. This is followed by the water-gas shift reaction, which converts CO into CO_2 while generating additional hydrogen. While these two reactions define the system at equilibrium, the process typically operates far from equilibrium [44]. SMR takes place in tubular reactors (10–13 m long, 100 mm in diameter) at temperatures of 700–1000 °C and pressures of 15–50 bar, with catalyst pellets enhancing reaction efficiency. Heat is supplied externally by burning fuel gas with air in furnace burners surrounding the reactor tubes [45,46].

Catalyst selection is critical, influencing reaction efficiency, heat transfer, and pressure drop while also being a key cost factor [47,48]. Beyond the physical properties of pellet shape and size, catalytic performance is influenced by active metals, promoter effects, support materials, particle size, and metal coordination states. While noble metals (Ru, Rh, Pd, Pt) exhibit high activity and low carbon deposition, their high cost limits widespread industrial use. Instead, nickel-based catalysts are preferred for their affordability, with optimal particle sizes of 2–3 nm minimizing carbon formation [49–51]. Secondary metals such as Fe can further enhance catalytic performance [49]. Catalyst deactivation occurs through chemical, thermal, or mechanical mechanisms. Chemical deactivation includes poisoning, where impurities such as H_2S or strongly adsorbed species block active catalytic sites, as well as fouling due to coke or carbon deposits from hydrocarbon cracking or condensation reactions [42,49,52].

Industrial SMR processes typically employ fixed-bed reactors [52], producing gas compositions of 75–80% H_2, 20–25% CO_2, and 0.5–2% CO [53]. To minimize emissions, carbon capture is essential, while hydrogen purification is necessary for various applications. Separation technologies include both chemical and physical methods, with pressure swing adsorption (PSA) being the most widely used, achieving purities of 96–99.999% [53,54].

This study evaluates the potential of AD and SMR to convert agricultural kiwifruit and apple waste into low-carbon hydrogen, aligning with New Zealand's goal of achieving net-zero emissions by 2050. A circular economy approach is explored that not only reduces landfill dependency but also

 doi:10.20944/preprints202602.1296.v1

provides biofertilizers, decreases reliance on imported fossil fuels, and enhances energy security. Furthermore, the effectiveness of using a low-cost, readily available biological catalysts, such as cow manure, is investigated. This research contributes to the development of sustainable energy solutions, and offers valuable insights for industries seeking a alternative to fossil-based hydrogen production pathways. The proposed process is illustrated in Figure 1 and involves the production of a biogas intermediate via AD and subsequesnt conversion of the produced biomethane to hydrogen via a SMR process.

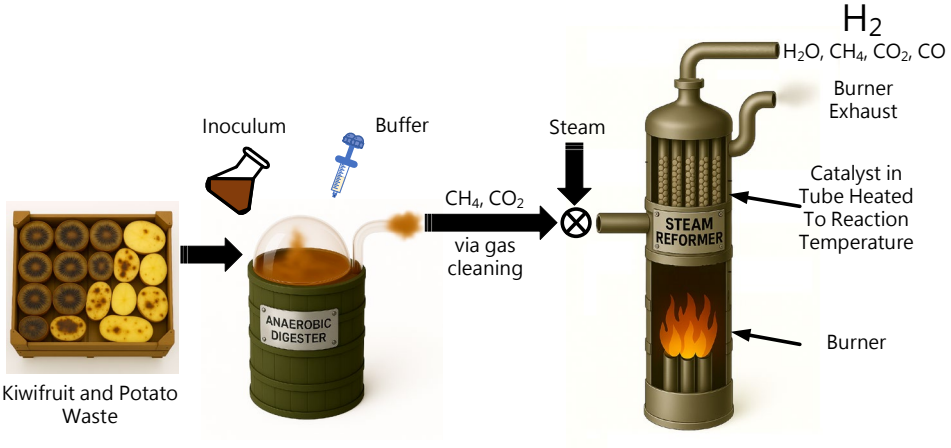

Figure 1. Process overview of production of hydrogen using methane produced by kiwifruit and potato waste.

To achieve this, the study follows a structured approach, beginning with a detailed physicochemical analysis of the feedstock and inoculum to assess key parameters influencing process efficiency. Biomethane potential (BMP) tests are conducted to evaluate methane production from different feedstock mixtures, while gas composition analysis provides insights into fermentation dynamics and carbon conversion efficiency. Finally, the SMR process is examined through theoretical simulations to estimate hydrogen yield and assess potential catalyst deactivation issues, establishing the feasibility of biomethane as a feedstock.

2. Materials and Methods

2.1. Substrate and Inoculum Analysis

Kiwi fruits and apples were used in two different feedstock mixtures. Given the high degradability of pure fruit, it was hypothesized that using it as a feedstock could lead to acidification during anaerobic digestion. To mitigate this, the addition of potatoes was investigated. Mixture 1 consists of a 50:50 ratio of kiwi fruit to apples, and mixture 2 contains kiwi fruit, apples, and potatoes in a 40:40:20 ratio. Potatoes, being rich in starch, decompose more slowly and were expected to promote a more balanced degradation process, stabilizing the pH. For each analysis or experiment, all ingredients were purchased fresh from local grocery stores in Hamilton, New Zealand. The fruits were not washed before processing, chopped to achieve the desired weight ratios, and blended until smooth, with an additional minute of blending to standardize consistency.

Cow manure was used as the inoculum and collected from a local cow paddock (Baverstock Rd, Brymer Rd, Hamilton, New Zealand). To ensure freshness, manure was gathered in the form of fresh cow pats in the morning before each experiment. After collection, the manure was thoroughly mixed before use in experiments.

The mixed inoculum and blended feedstock samples were characterized by total solids (TS), volatile solids (VS), and ash content by APHA method 2540 B and 2540 E using a FHX-14 Daihan Scientific muffle furnace. Alkalinity was determined using the Alkaphot Palintest (0-500 mg/L $CaCO_3$), freshly blended feedstock samples were diluted 100- to 200-fold, and measurements were

 doi:10.20944/preprints202602.1296.v1

performed using program 02 (Total Alkalinity) on the Palintest Photometer 7500 Bluetooth. Ammonium content was measured using the Palintest program 62 (Ammonium). Freshly blended samples were diluted at ratios of 1:100 or 1:150 to ensure the readings fell within the test range (0–100 mg/L NH_4). For Total Sulfur (TSu), Total Phosphorus (TP), trace elements, Chemical Oxygen Demand (COD), Total Carbon (TC), and Total Nitrogen (TN), different sample preparation methods were applied. Inoculum samples were dried and ground, while feedstock samples were freeze-dried and homogenized using a ball mill at 27 1/s for 20 seconds. COD was measured using high-range Hach digestion vials (20–1,500 mg/L). TSu, TP, and trace elements in the feedstock were analyzed via inductively coupled plasma mass spectrometry (ICP-MS) using an Agilent ICP-QQQ 8900 system. TN and TC analyses were outsourced to Lincoln University and conducted using an Elementar Analyzer.

2.2. Biochemical Methane Potential (BMP) Assay

BMP tests were conducted using batch experiments with a volume displacement setup, incorporating a CO_2 scrubber. The experimental system consisted of 1 L Schott bottles as digesters and a CO_2 scrubber, and 1.5 L water bottles for gas measurement (Figure 2). Each bottle cap was modified by drilling two holes to accommodate shortened 1 mL syringes, which were affixed with epoxy to ensure an airtight seal. Gas flow into the NaOH and water bottles was facilitated by inserting tubing through one of the syringes and securing it with adhesive. All bottles were interconnected using 3 mm PVC tubing.

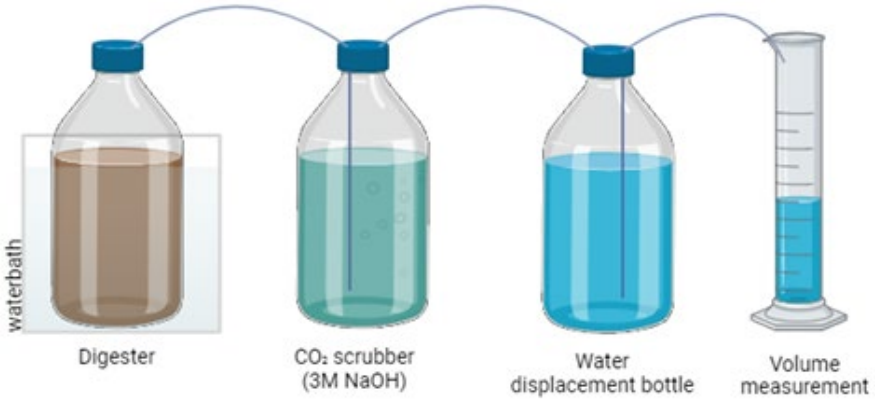

Figure 2. BMP test apparatus with the digester bottle submerged in a water bath (artwork created in BioRender.com).

The two different feedstock mixtures were tested under the conditions summarized in Table 1, following a protocol adapted from Angelidaki et al. [55]. Before each experimental run, the system was sealed with heavy-duty thread seal tape and pressure tested by injecting air and verifying that pressure remained stable. To eliminate residual oxygen, the headspace was flushed with nitrogen. Digesters were incubated at 38 ± 1 °C in a water bath. Once a day, all digesters were manually shaken, and the temperature in the gas phase of the water displacement bottle, along with the displaced water volume, was recorded. Methane volumes were adjusted to standard conditions (273.15 K, 1 atm). Each experimental condition was conducted in triplicates, with triplicate blank experiments to account for the inoculum itself. The obtained data was processed in Microsoft Excel 2501.

Table 1. Experimental parameters.

Parameter	Feedstock mixture 1[1]	Feedstock mixture 2[2]
Working volume (mL)	750	750
Headspace volume (mL)	616	616
Temperature (°C)	37 ± 1	37 ± 1

 doi:10.20944/preprints202602.1296.v1

Starting pH	7.0 - 7.1	7.0 - 7.1
Buffer, concentration (g/L)	Na_2CO_3, 1.5	Na_2CO_3, 1.5
ISR[3]	2 & 4	2 & 4
Loading inoculum (g)	86 & 80	79 & 79
Loading substrate (g)	32 &15	30 & 15
OLR (gVS)[4]	14.1 & 10.9	12.9 & 10.8
OLR (gCOD)[5]	16.5 & 13.1	15.5 & 13.1
Mixing	manual shaking once a day	manual shaking once a day
Number of replicates	3 per condition	3 per condition
Duration (d)	30	30

[1] 50:50 Kiwi:Apple, [2] 40:40:20 Kiwi:Apple:Potato, [3] Inoculum-to-substrate ratio (VSinoculum/VSsubstrate), [4] Organic loading rate in g volatile solids, [5] Organic loading rate in g chemical oxygen demand.

2.2.1. System Optimization / Validation

Trial tests revealed an initial increase in displaced water that stagnated over the first night, likely due to gas expansion and degassing during temperature equilibration. Control experiments with water-filled digester bottles at different temperatures (4 °C, room temperature, and 35 °C) confirmed this hypothesis, as water displacement only occurred in the first two. These findings underscore the necessity of preheating the digester contents before BMP startup to prevent measurement artifacts.

In literature, an optimal range of initially loaded VS is recommended. While Holliger et al. mention a total volatile solids concentration between 20 and 60 gVS/L [56], Ohemeng-Ntiamoah et al. recommend a substrate loading range of 10 to 60 gVS/L, while ensuring that the mass of inoculum exceeds the substrate mass [57]. However, adhering to these recommendations led to severe foaming, which pressurized the digester bottles. Reducing the working volume and organic loading to 10–20 gVS/L effectively mitigated this issue.

2.3. Theoretical Maximum Methane Yield

The chemical formula of both feedstock mixtures was determined, from which the theoretical maximum biomethane yield (TMBY) was calculated based on the following formula, developed by Buswell and Mueller [58]:

$$CnHaOb + \left(n - \frac{a}{4} - \frac{b}{2}\right) H2O \rightarrow \left(\frac{n}{2} - \frac{a}{8} + \frac{b}{4}\right) CO2 + \left(\frac{n}{2} + \frac{a}{4} - \frac{b}{8}\right) CH4 \quad (1)$$

This model neglects factors like inhibition due to ammonia or hydrogen sulfide contamination of biogas, and will deviate from experimental data due to certain assumptions and the dynamic nature of AD.

The theoretical maximum methane yield of the feedstock mixtures was determined based on the biochemical composition of the individual feedstock components. The moisture content, as well as the fractions of carbohydrates, crude protein, and crude fat were taken from literature for kiwifruit [59], apple [60], and potato [61] separately. The mass of each feedstock component was calculated based on the total input mass and fruit ratios per experiment. These masses were multiplied by the respective carbohydrate, fat, and protein fractions to obtain the mass of each biochemical component. Assuming average elemental compositions, as shown in Table 2, molecular weights were calculated, and the corresponding molar amounts were determined by dividing each component's mass by its molecular weight.

Table 2. Elemental composition of biochemical fractions.

	Carbon C	**Hydrogen H**	**Oxygen O**	**Nitrogen N**
Molecular weight (g/mol)	12	1	16	14

 doi:10.20944/preprints202602.1296.v1

Carbohydrate	6	12	6	0
Protein	4	6	1	1
Fat	16	31	2	0

From these values, the moles of individual elements (C, H, O, and N) were calculated by multiplying the number of moles of each biochemical fraction by the number of carbon, hydrogen, oxygen, and nitrogen atoms present in its molecular structure. By summing the moles of element across all fractions, the total moles of carbon in the input feedstock mass were determined. The number of methane and carbon dioxide moles were determined using the following relationships:

$$\boldsymbol{n(CO2)} = \frac{\boldsymbol{n(C)}}{\boldsymbol{2}} - \frac{\boldsymbol{n(H)}}{\boldsymbol{8}} + \frac{\boldsymbol{n(O)}}{\boldsymbol{4}} \quad (2)$$

$$\boldsymbol{n(CH4)} = \frac{\boldsymbol{n(C)}}{\boldsymbol{2}} + \frac{\boldsymbol{n(H)}}{\boldsymbol{8}} - \frac{\boldsymbol{n(O)}}{\boldsymbol{4}} \quad (3)$$

By multiplying their respective moles by their molecular weights, the masses of CH_4 and CO_2 were then obtained. The volume of each gas was calculated by dividing its mass by its respective density, as described in Formula x. The resulting volumes of CH_4 and CO_2 were then summed for each feedstock mixture and ISR condition.

$$\boldsymbol{V(biogas)} = \frac{\boldsymbol{n(CO2)} * \boldsymbol{MW(CO2)}}{\boldsymbol{\rho(CO2)}} + \frac{\boldsymbol{n(CH4)} * \boldsymbol{MW(CH4)}}{\boldsymbol{\rho(CH4)}} \quad (4)$$

2.4. Steam Methane Reforming (SMR) Modeling and Simulation

The feasibility of using biomethane as a feedstock for SMR was analyzed through a novel 3D dynamic simulation in COMSOL Multiphysics, with a focus on assessing the performance of a nickel-based catalyst and the overall viability of hydrogen production from biomethane as an alternative to natural gas. Detailed reaction engineering, physics-based modeling, and an evaluation of deactivation mechanisms such as sulfur poisoning were incorporated. Boundary conditions based on physics applying to the steam reformer must be set to account for heat losses, material properties, and gas flow behavior, creating an accurate representation of real-world SMR conditions. The transport of concentrated species was defined to model diffusion over the catalyst bed accurately. The inlet temperature into the porous media was set at 925 K. The values for the tube alloy wall thermodynamic properties used in the COMSOL simulation was derived from Lao et al. 2016 [62].

For Darcy's Law, the permeability of the porous media was calculated as $1 * 10^{-9}$ m^3, with inlet and outlet pressures of 16.64 bar and 16.57 bar, respectively. Heat transfer in fluids used the same heat transfer coefficient as the tubes, as heat was transferred from the burner to the tubes. The burner inlet temperature was 1220 K, with heat transfer occurring between the burner and the surrounding atmosphere.

The reactions taking place in the reformer tubes are

$$CH_4 + H_2O \rightleftharpoons CO + 3H_2 \; \Delta H^o_{298} = 206 \; kJ/mol$$
$$CO + H_2O \rightleftharpoons CO_2 + H_2 \; \Delta H^o_{298} = -41.4 kJ/mol$$
$$C_2H_6 + 2H_2O \rightleftharpoons 2CO + 5H_2 \; \Delta H^o_{298} = -84.7 \; kJ/mol$$
$$C_3H_8 + 3H_2O \rightleftharpoons 3CO + 7H_2 \; \Delta H^o_{298} = -103.85 \; kJ/mol$$
$$C_4H_{10} + 4H_2O \rightleftharpoons 4CO + 9H_2 \; \Delta H^o_{298} = -126.2 \; kJ/mol$$

The basis of the SMR kinetics is the Langmuir-Hinshelwood-Hougen-Watson (LHHW) model for reactions taking place on the surface of a catalyst. The kinetics for the methane formation was taken from Xu and Froment [70]. Whilst the higher order hydrocarbon reaction kinetics was taken from Seong [71].

Implementation in COMSOL was by way of three-dimensional finite element-based model of the tube reactor and burner section. The tube was modelled using physics for transport of concentrated species, heat transfer in porous media and Darcy's Law. For the burner section, the

 doi:10.20944/preprints202602.1296.v1

physics used were heat transfer in fluids and laminar flow. The tube length comprised of the full length of the catalyst in the reactor thus effectively implementing a tubular plug flow reactor.

To factor in the reduction in catalyst performance due to carbon deposition, a first order kinetic expression for change in porosity ε was implemented according to $d\varepsilon/dt=-k_{por}\varepsilon$ which gave a rate constant of 0.03/year. This was the basis for the calculation of 5-year catalyst performance. Similarly, the reduction in catalyst lifetime due to sulfur poisoning was based on model of Rostrup-Neilsen [72].

To estimate hydrogen yields the hydrogen mole fraction was taken at the outlet of the tubular reactor section from a steady-state simulation.

2.5. Ideation of Graphical Content

The process of creating the icon illustrations contained in Figure 1 such as the feed and unit operations was AI generated, created in ChatGPT through a series of prompts. These prompts were iterative in nature with emphasis on conceptualising a graphic that illustrates the formation and passage of biomethane through the process to the end product being hydrogen.

3. Results

3.1. Substrate and Inoculum Analysis

The physicochemical characteristics of the two feedstocks and the inoculum are presented in Table 3. Both feedstocks exhibited high moisture content, with 84.3% for Feedstock 1 (Fs1) and 83.1% for Feedstock 2 (Fs2), which is typical for fruit-based substrates. The inoculum also exhibited a high moisture content of 85.3%, which supports microbial distribution and improves substrate accessibility. Its total solids content was measured at 14.7%, with a volatile solids fraction of 11.5%, representing a considerable amount of readily degradable organic matter. The total solids content of Fs1 and Fs2 was 15.6% and 16.9%, respectively, while volatile solids were 15.2% and 16.6%. The high VS fractions indicate a substantial amount of biodegradable organic matter, supporting their potential for efficient biogas production. The feedstocks displayed acidic pH values, which can be attributed to the natural acidity of kiwifruit. In contrast, the inoculum exhibited a slightly alkaline pH, which is favorable for stabilizing the digestion process. Alkalinity plays a critical role in maintaining pH stability within the digester. In Fs1 it was measured at 5,222 mg/L $CaCO_3$, in Fs2 6,236 mg/L $CaCO_3$. Notably, the inoculum had a substantially higher alkalinity of 13,605 mg/L $CaCO_3$, highlighting its strong buffering capability which helps stabilize digestion conditions. Chemical oxygen demand, which represents the total oxidizable organic content, was measured at 150 mg/g WM for Fs1 and 152 mg/g WM for Fs2. The COD of cow manure was also substantial with 154 mg/g WM, providing an additional source of biodegradable matter in the system, enhancing the total digestion potential.

Table 3. Physical and chemical properties of feedstock and inoculum.

Characteristic	Feedstock 1[1]	Feedstock 2[2]	Inoculum
Volatile solids (%)	15.2	16.6	11.5
Total solids (%)	15.6	16.9	14.7
Moisture content (%)	84.3	83.1	85.3
pH (-)	3.44	3.83	8.43
Alkalinity (mg/L $CaCO_3$)	5,222	6,236	13,605
Ammonium (mg/L NH_4)	18.5	24.8	194
Chemical Oxygen Demand (mg/g WM)[3]	150	152	154

[1] 50:50 Kiwi:Apple, [2] 40:40:20 Kiwi:Apple:Potato, [3] Per wet mass.

Macro- and micronutrient concentrations obtained by ICP-MS are reported in Table 4. Macronutrients such as carbon, nitrogen, phosphorus, sulfur, potassium, and calcium are

 doi:10.20944/preprints202602.1296.v1

fundamental for microbial metabolism during digestion. Fs 1 contained 39.9% total carbon and 0.40% total nitrogen, resulting in a C/N ratio of 99.9, while Fs 2 showed 39.4% carbon and 0.66% nitrogen, corresponding to a C/N ratio of 58.9. These values indicate a potential nitrogen deficiency, particularly in feedstock mixture 1. Furthermore, Fs 1 contained 0.1079% phosphorus and 0.0541% sulfur, and Fs 2 0.0171% phosphorus and 0.0877% sulfur. Potassium levels were higher, with 1.19% in Fs 1 and 1.65% in Fs 2, suggesting adequate availability for microbial activity. Trace levels of micronutrients, including manganese, zinc, copper, cobalt, molybdenum, and selenium, were detected in both substrates. Importantly, heavy metals such as cadmium, mercury, arsenic, and lead were either absent or detected at negligible concentrations, minimizing the risk of toxicity or long-term accumulation within the digestion system.

Table 3. Elemental composition of feedstock mixtures.

Characteristic*	Feedstock 1	Feedstock 2
Total Carbon of DM (%)	39.9	39.4
Total Nitrogen of DM (%)	0.40	0.66
C/N ratio on DM basis	99.9	58.9
Total Phosphorus of DM (%)	0.1079	0.0171
Total Sulfur of DM (%)	0.0541	0.0877
Total Potassium of DM (%)	1.1872	1.6455
Total Calcium of DM (%)	0.1113	0.0566

*Values are reported on a dry matter basis.

Taken together, these results confirm that both the feedstock mixtures and the inoculum exhibit favorable characteristics for anaerobic digestion. The feedstocks offer high levels of easily degradable organic matter and adequate buffering capacity to counteract their inherent acidity, alongside low ammonia concentrations and a beneficial profile of macro- and micronutrients. Notably, feedstock mixture 2 shows stronger potential for biogas production due to its more balanced nutrient composition. Concurrently, the inoculum provides essential qualities such as high moisture content, substantial organic matter, and sufficient buffering capacity, forming a solid foundation for stable and efficient digestion performance.

3.2. Biochemical Methane Potential (BMP) Assay

The results of the BMP tests for both feedstock mixtures at different inoculum-to-substrate ratios are presented in Table 5. Under ISR 4 conditions, approximately 2.2 g VS of substrate were applied, while ISR 2 conditions involved nearly double the input, with 4.3-4.7 g VS. Volatile solids destruction was low in three of the four conditions. Fs1 at ISR 2 and ISR 4, as well as Fs2 at ISR 2, all exhibited rates around 9-10%. In contrast, Fs2 under ISR 4 achieved a notably higher VS destruction of 50.1%, indicating substantially improved degradability under these conditions. A similar trend was observed in the carbon conversion efficiencies. For Fs1, ISR 2 and ISR 4, and Fs2 at ISR 2, around 8-10% of the initial carbon from the substrate was converted into carbon in gaseous products (methane and CO_2). In comparison, Fs2 under ISR 4 showed a markedly higher carbon conversion of 46.5%.

The accumulated methane volumes further support this trend. Fs1 under ISR 2 and Fs2 under ISR 2 produced 249.5 and 207.2 NmL of methane, respectively, while Fs1 under ISR 4 generated only 136.1 NmL. Once again, Fs2 under ISR 4 significantly outperformed all others, with a total methane production of 481.9 NmL. In terms of BMP values, Fs2 under ISR 4 again stands out, reaching 44.7 NmL CH_4/gVS, which is more than double the yield of any other condition, which ranged from 12.5 to 17.7 NmL CH_4/gVS.

Moreover, the theoretical maximum biomethane yields calculated from feedstock composition were consistently higher under ISR 2 conditions across both feedstocks, with 161.7 and 199.2 mLCH_4/gVS for Fs1 and Fs2, respectively, compared to ISR 4 with 98.2 and 118.5 mLCH_4/gVS. This is expected, as a lower ISR introduces more organic material per unit of inoculum, thereby increasing

 doi:10.20944/preprints202602.1296.v1

the theoretical methane potential. A notable discrepancy of approximately a factor of 10 was observed when comparing BMP results to TMBY. This difference reflects the well-known gap between idealized theoretical potentials and actual process performance, but also implies that there is room fro optimization of BMP test conditions. Theoretical values assume complete degradation and conversion of all organic matter into methane under optimal conditions, which is rarely achieved in practice due to microbial maintenance requirements, substrate recalcitrance, biomass synthesis, and operational limitations.

In summary, the results confirm that both feedstock composition and inoculum-to-substrate ratio play a crucial role in methane production. Although overall methane yields, carbon conversion, and VS destruction were moderate to low, the condition Fs2 at ISR 4 showed the best performance, suggesting potential benefits from even higher ISR values. Importantly, the successful generation of biogas in this initial study demonstrates the viability of agro-industrial kiwi and apple waste as a feedstock. With further research and process optimization, significantly improved methane yields may be achievable.

Table 4. Biomethane potential analysis findings.

Sample	VS from Substrate (g)	VS destruction of Substrate (%)	Carbon Conversion (%)	Accumulated Methane (NmL)[1]	BMP ($NmLCH_4/gVS$)	TMBY ($mLCH_4/gVS$)
Fs1,ISR2	4.7	9.70	9.74	249.5	17.7	161.7
Fs1,ISR4	2.2	10.1	10.1	136.1	12.5	98.2
Fs2,ISR2	4.3	8.66	8.05	207.2	16.0	199.2
Fs2,ISR4	2.2	50.1	46.5	481.9	44.7	118.5

[1] NmL have been adjusted to standard pressure of 1 atm and a temperature of 273.15 K.

3.3. Steam Methane Reforming (SMR) Modelling and Simulation

The performance characteristics of the SMR process comparing biomethane and natural gas are summarized in Table 6. As expected for SMR, substantial heat input is required to sustain reaction rates and maintain conversion efficiency. The heat of reaction for biomethane was calculated at 30.2 kW/m^3, slightly lower than the 32 kW/m^3 required for natural gas. This difference is attributed to the absence of higher-order hydrocarbons in biomethane, which typically demand additional energy for reforming.

Catalyst deactivation due to sulfur poisoning is a critical limitation in biomethane reforming. The simulated sulfur coverage on the catalyst surface reached 95%, indicating near-complete deactivation. In comparison, natural gas showed a sulfur coverage of 69%, suggesting that while both fuels pose a risk of catalyst poisoning, the threat is more severe with biomethane. While biomethane presents a greater risk of sulfur poisoning, natural gas is more prone to coke formation due to the presence of higher-order hydrocarbons, which crack more readily, contributing to the porosity loss of the catalyst and additional long-term performance degradation.

Table 5. SMR performance characteristics.

Characteristic	Biogas	Natural Gas
Heat of reaction (kW/m^3)	30.2	32
Sulfur coverage (%)	95	69
Outlet concentration of H_2 (mol/m^3)	91	86
Conversion efficiency (%)	46	43

Figure 3, supported by the data presented in Table 7, illustrates the molar concentration profiles of key gas components along the reactor length. Although the inlet compositions for both natural gas and biomethane were identical in the simulation, the outlet hydrogen concentration was higher for biomethane at 91 mol/m^3 compared to 86 mol/m^3 for natural gas, confirming its high suitability for

 doi:10.20944/preprints202602.1296.v1

hydrogen production. Despite this advantage, the methane conversion efficiency for biomethane reached only 46%, and 43% for natural gas indicating potential for further optimization of process parameters to enhance methane utilization and hydrogen output.

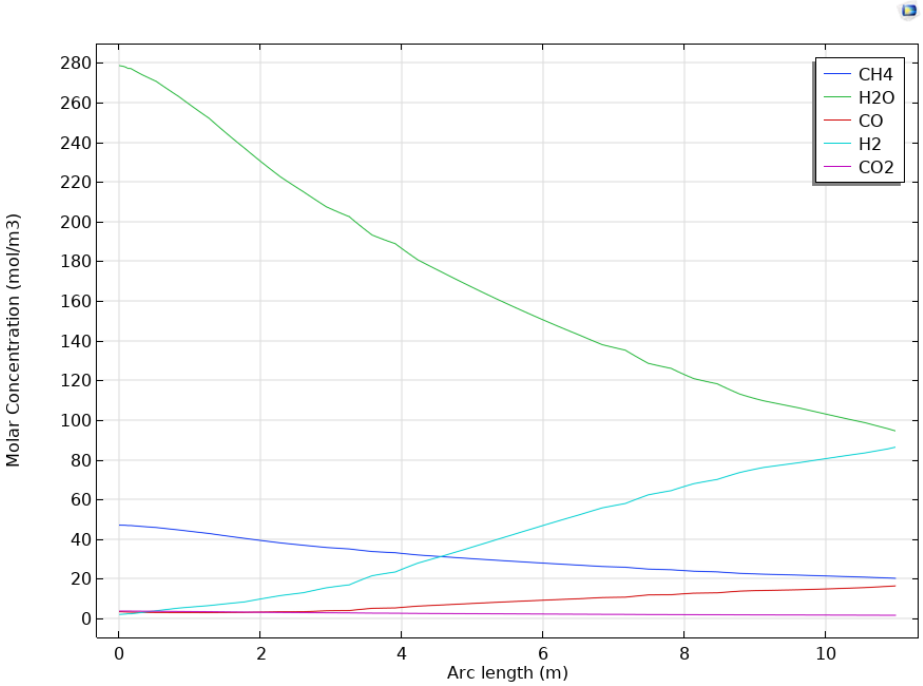

Figure 3. Molar concentration over reactor length.

Simulations over a five-year operational period reveal notable differences in catalyst performance and gas composition for SMR using biomethane versus natural gas, as shown in Table 7. With a fresh catalyst, both feedstocks yield comparable hydrogen concentrations, with 69.1 mol% for biomethane and 69.3 mol% for natural gas. However, after five years, hydrogen output declines more sharply for biomethane, dropping to 44.8 mol% compared to 57.0 mol% for natural gas. Methane slip nearly doubles in the biomethane case, from 16.7 to 39.5 mol%, while it increases more moderately in natural gas reforming from 16.2 to 26.6 mol%. Similarly, CO_2 levels rise significantly for biomethane, from 1.13 to 3.22 mol%, but only slightly for natural gas, from 1.31 to 1.81 mol%. These results highlight the need for effective sulfur removal strategies when reforming biomethane.

Table 6. Comparison of outlet gas composition.

	Characteristic	Biogas	Natural Gas
New Catalyst	H_2 (mol%)	69.1	69.3
	CO_2 (mol%)	1.13	1.31
	CO (mol%)	12.8	13.2
	CH_4 (mol%)	16.7	16.22
Five-year-old Catalyst	H_2 (mol%)	44.8	57.0
	CO_2 (mol%)	3.22	1.81
	CO (mol%)	12.3	14.5
	CH_4 (mol%)	39.5	26.6

Overall, the molar concentration profiles highlight biomethane's strong potential as a feedstock for hydrogen production via SMR. Compared to natural gas, biomethane reforming is more energy-efficient, requiring lower heating input, and poses a lower risk of coke formation. However, its long-term operational stability is more vulnerable to sulfur poisoning.

4. Discussion

 doi:10.20944/preprints202602.1296.v1

4.1. Substrate and Inoculum Analysis

The physicochemical properties of the feedstocks and inoculum provide important insights into their suitability for anaerobic digestion and their potential to support stable and efficient biogas production. Notably, the alkalinity levels measured in both feedstock mixtures exceeded within the typical range reported for anaerobic digesters, which is between 1,500–5,000 mg/L [63]. This elevated buffering capacity is particularly beneficial given the acidic starting pH of the mixtures, offering protection against acidification during the hydrolytic and acidogenic phases. Ammonium concentrations in both mixtures remained well below inhibitory levels commonly reported at 1,500–3,000 mg/L at a pH higher than 7.4 [64], ensuring that methanogenic activity would not be adversely affected.

The COD content of both feedstock mixtures was comparable, but the actual loading concentrations of 3.10-6.61 g/L were modest relative to other studies. For instance, Dhar et al. used initial loadings of 5.1, 10.4, and 15.2 g/L COD, yielding 9.3, 10.7, and 17.7 L of biogas [65]. This suggests that while the feedstocks possess reasonable biodegradability, the relatively low organic loading in this study may have limited their maximum methane potential. Future experiments could explore higher loading rates to assess yield improvements.

The C/N ratios observed in both Fs1 (99.9) and Fs2 (58.9) were markedly above the optimal range, with values ranging from 20:1 to 30:1 for methanogenesis and 10:1 to 45:1 for hydrolysis [28]. While such ratios minimize ammonia toxicity, they may lead to nitrogen deficiency, impairing microbial growth and slowing methane production. Future studies should investigate nitrogen supplementation or co-digestion with nitrogen-rich substrates to restore balance and enhance biodegradability. A nutrient comparison with a standard supplementation strategy based on Du Preez et al. [66] revealed that potassium levels were sufficient. In contrast, phosphorus concentrations (7–12 mg/L) were markedly lower than the recommended 60 mg/L, suggesting a potential nutrient limitation. To address this, targeted phosphorus supplementation—aligned with microbial demand—could enhance digestion performance while minimizing the risks associated with nutrient oversupply. Nonetheless, any supplementation strategy must carefully consider microbial requirements, the potential inhibitory effects of excess nutrients, and economic feasibility. It is also important to note that elemental analysis reflects total nutrient content but does not necessarily indicate bioavailability, which may be affected by processes such as precipitation and adsorption within the digester matrix.

Finally, the inoculum exhibited characteristics of high-quality seeding material, as per Hollinger et al. [56]. The measured alkalinity exceeds 3,000 mg/L, the threshold characteristic of high-quality inoculum for BMP testing, confirming its robust buffering capacity. The pH falls within the optimal range of 7.0 to 8.5 for methanogenic activity, as recommended. Additionally, the ammonium concentration is well below the suggested upper limit of 2,500 mg/L, reducing the risk of ammonia inhibition and further confirming the inoculum's suitability for anaerobic digestion.

Overall, the nutrient profiles, buffering capacity, and organic content of both the feedstocks and the inoculum confirm their fundamental suitability for anaerobic digestion. These characteristics support the potential of agro-industrial kiwifruit and apple waste as promising resources for low-carbon hydrogen production.

4.2. Biochemical Methane Potential (BMP) Assay

The BMP tests were conducted to evaluate the anaerobic biodegradability and methane potential of agro-industrial kiwifruit and apple waste. Results indicate that both the feedstock composition and the inoculum-to-substrate ratio significantly influenced methane production. Among the tested conditions, the feedstock F2 at ISR 4 achieved the highest methane yield, reaching up to 45 mL CH_4/g VS.

For comparison, Kawai et al. reported methane yields of 435 mL CH_4/g VS for food waste at ISR 3, and 269mL CH_4/g VS at ISR 2 [66], supporting the trend observed in this study that higher an ISR enhances digestion performance. However, these reported yields are approximately ten times higher

 doi:10.20944/preprints202602.1296.v1

than the ones achieved in this study. Similarly, a review by Ohemeng-Ntiamoah et al. indicates that methane yields for comparable substrates typically range between 400-500 mL CH_4/g VS, with some studies reporting values closer to 100 mL CH_4/g VS [57], highlighting the substantial variability depending on feedstock characteristics and process conditions.

A study by Hull-Cantillo et al. reported volatile solids destruction rates between 47-53% during BMP tests with liquid dairy effluent sludge [67]. In comparison, only condition F2,4 in the present study reached a similar range, while the others showed considerably lower VS removal, suggesting suboptimal digestion. Similarly, Gao et al. investigated the anaerobic digestion of wheat straw and reported a VS degradation rate of 50.13% by day 24, alongside a detailed carbon flow analysis that revealed 49.96% of initial carbon was converted to biogas, 44.43% retained in the solid digestate, and 5.61% in the liquid phase [68]. Again, only the carbon conversion efficiency of F2,4 align well with those findings, indicating favorable digestion performance under optimized ISRs. In contrast, lower conversion rates in the other experiments may point to early acidification, resulting in incomplete substrate utilization

Despite the comparatively low yields in this study, the results underline the potential of the tested feedstocks for biogas production, though significant improvements are needed. Enhancing the buffering system and supplementing key nutrients, especially nitrogen and phosphorus, which were shown to be deficient, may improve digestion efficiency. Nonetheless, nutrient addition should be carefully tailored to microbial demand, as unspecific supplementation could negatively impact process stability or increase costs. Future studies should furthermore investigate whether increasing the ISR can effectively stabilize the process and enhance methane generation.

Other possible reasons for limited methane production include the accumulation of volatile fatty acids, which were not measured in this study, or the presence of inhibitory compounds such as pesticide residues or preservatives in fruit waste. While no heavy metals were detected in the feedstock mixtures, the presence of unidentified inhibitors cannot be ruled out. Should further optimization efforts, including nutrient supplementation and improved buffering, not yield significant improvement, the quality or microbial activity of the inoculum itself may be the primary limiting factor.

Overall, this study lays essential groundwork for evaluating the anaerobic digestion potential of kiwifruit and apple waste. The inclusion of potato in Fs2 appears to serve its purpose as a co-substrate that moderates acidification and improves the C/N ratio, contributing to more stable digestion dynamics. These initial findings underscore both the feasibility and the challenges of using these agro-industrial residues for biogas production, pointing to the need for further optimization in substrate formulation, nutrient supplementation, and inoculum quality to unlock their full potential.

4.3. Steam Methane Reforming (SMR) Simulation

Consequently, biomethane reforming is more energy-efficient and requires less heating compared to natural gas. In theory, this improved efficiency could enable the use of shorter reformers, thereby reducing equipment costs. However, these assumptions require validation through experimental or industrial-scale studies.

Biomethane shows strong potential for hydrogen production, yielding 91 mol/m^3 H_2 compared to 86 mol/m^3 from natural gas. However, its current methane conversion efficiency of 46% indicates room for improvement. Studies suggest that optimizing conditions such as residence time, steam-to-carbon ratio, temperature, and pressure could raise conversion efficiency to nearly 90% [69].

5. Conclusions

In conclusion, this research contributes to the growing body of knowledge on low-carbon hydrogen production and highlights the viability of biohydrogen as a renewable energy carrier. While the results reflect early-stage process development, they demonstrate the potential of agro-industrial residues, specifically kiwifruit and apple waste, as viable feedstocks for anaerobic digestion and subsequent hydrogen generation via steam methane reforming. The findings provide

 doi:10.20944/preprints202602.1296.v1

a valuable starting point for industries aiming to reduce their reliance on fossil fuels. Hydrogen-producing companies stand to benefit from adopting waste-to-hydrogen pathways, especially in regions like New Zealand, where agricultural residues are both plentiful and currently rather underexploited. To fully realize this potential, further research into process optimization will be essential.

Author Contributions: Conceptualization, E.B. and P.K.; Methodology, E.B.; Software, P.K.; Validation, E.B., and P.K.; Formal analysis, E.B.; Investigation, E.B.; Writing—original draft preparation, E.B.; Visualization, E.B.; Writing—review and editing, P.K.; Supervision, P.K. All authors have read and agreed to the published version of the manuscript.

Funding: This research received no external funding.

Data Availability Statement: Data is contained within the article.

Acknowledgments: We acknowledge the technical staff at the University of Waikato for assisting with this research. We acknowledge ChatGPT for producing icon graphics in the illustrations presented in this paper.

Conflicts of Interest: The authors declare no conflicts of interest.

References

1. *About the horticulture industry in New Zealand*. 07.01.2025]; Available from: https://www.hortnz.co.nz/about-us/.
2. *Kiwifruit Book*. 2022, NZKGI New Zealand Kiwifruit Grower. p. 37-48.
3. *Apple and Pears - The Market*. 08.01.2025]; Available from: https://www.tupu.nz/en/fact-sheets/apples-and-pears/.
4. *Apple Thinning 2024*. 08.01.2025]; Available from: https://www.bostock.nz/news/apple-thinning-2024.
5. *Growing and Orchard Management*. 07.01.2025]; Available from: https://www.whitehallfruitpackers.co.nz/page/growing-and-orchard-management/.
6. *Waste sector emissions*. 08.01.2025]; Available from: https://environment.govt.nz/facts-and-science/waste/waste-sector-emissions/#about-waste-emissions-data.
7. Evro, S., B.A. Oni, and O.S. Tomomewo, *Carbon neutrality and hydrogen energy systems.* International Journal of Hydrogen Energy, 2024. **78**: p. 1449-1467.
8. *Climate Change Response (Zero Carbon) Amendment Bill*. 2019 24.02.2025]; Available from: https://www.legislation.govt.nz/bill/government/2019/0136/latest/LMS183736.html
9. Midilli, A. and I. Dincer, *Hydrogen as a renewable and sustainable solution in reducing global fossil fuel consumption.* International Journal of Hydrogen Energy, 2008. **33**(16): p. 4209-4222.
10. Mbie, A., *Vision for Hydrogen in New Zealand.* Energy Strategies for New Zealand. Availableat: https://www. mbie. govt. nz/building-and-energy/energy-and-natural-resources/energy-strategies-for-new-zealand/(Accessed on August 19, 2021), 2019.
11. Blasio, N.D. *The Colors of Hydrogen*. 2024 25.02.2024]; Available from: https://www.belfercenter.org/research-analysis/colors-hydrogen.
12. *Urgent action taken to bolster energy security*. 2024 25.02.2025]; Available from: https://www.beehive.govt.nz/release/urgent-action-taken-bolster-energy-security.
13. *H2 Stations Map*. 03.01.2025]; Available from: https://www.h2stations.org/stations-map/?lat=49.139384&lng=11.190114&zoom=2.
14. Cheng, S. and B.E. Logan, *Sustainable and efficient biohydrogen production* via *electrohydrogenesis.* Proceedings of the National Academy of Sciences, 2007. **104**(47): p. 18871-18873.
15. Wang, L., et al., *Evaluation of low-cost cathode catalysts for high yield biohydrogen production in microbial electrolysis cell.* Water Science and Technology, 2011. **63**(3): p. 440-448.
16. Chakraborty, A., et al., *Microbial electrolysis cells for effective biohydrogen biogenesis from biowastes*, in *Advances in Environmental Electrochemistry*. 2024, Elsevier. p. 55-87.

 doi:10.20944/preprints202602.1296.v1

17. Noori, M.T., et al., *Hydrogen production in microbial electrolysis cells with biocathodes.* Trends in Biotechnology, 2024. **42**(7): p. 815-828.
18. Hallenbeck, P.C. and J.R. Benemann, *Biological hydrogen production; fundamentals and limiting processes.* International journal of hydrogen energy, 2002. **27**(11-12): p. 1185-1193.
19. Ren, C., et al., *Pilot composite tubular bioreactor for outdoor photo-fermentation hydrogen production: from batch to continuous operation.* Bioresource Technology, 2024. **401**: p. 130705.
20. Goveas, L.C., et al., *Recent advances in fermentative biohydrogen production.* International Journal of Hydrogen Energy, 2024. **54**: p. 200-217.
21. Hawkes, F., et al., *Sustainable fermentative hydrogen production: challenges for process optimisation.* International journal of hydrogen energy, 2002. **27**(11-12): p. 1339-1347.
22. Humaira, A.H.A., et al., *Cell-Free Systems: Platform for Sustainable Commercial Biomanufacturing of Biochemicals.* Punjab University Journal of Zoology, 2024. **39**(2): p. 213-230.
23. Zhang, Y.P., J. Sun, and J.-J. Zhong, *Biofuel production by* in vitro *synthetic enzymatic pathway biotransformation.* Current opinion in biotechnology, 2010. **21**(5): p. 663-669.
24. Contreras, J., et al., *Catalysts for H2 production using the ethanol steam reforming (a review).* International Journal of Hydrogen Energy, 2014. **39**(33): p. 18835-18853.
25. Chen, W.-H., et al., *A critical and systematic review of sustainable hydrogen production from ethanol/bioethanol: Steam reforming, partial oxidation, and autothermal reforming.* Fuel, 2023. **333**: p. 126526.
26. Behera, S.S., P. Saranraj, and R.C. Ray, *Microbial bioethanol fermentation technologies—Recent trends and future prospects.* Biofuels and biorefining, 2022: p. 75-108.
27. Jahromi, A.F., et al., *Electrochemical promotion of ethanol partial oxidation and reforming reactions for hydrogen production.* Renewable energy, 2022. **183**: p. 515-523.
28. Wellinger, A., J.P. Murphy, and D. Baxter, *The biogas handbook: science, production and applications*. 2013: Elsevier.
29. Sihlangu, E., et al., *Investigating methane, carbon dioxide, ammonia, and hydrogen sulphide content in agricultural waste during biogas production.* Sustainability, 2024. **16**(12): p. 5145.
30. Meegoda, J.N., et al., *A review of the processes, parameters, and optimization of anaerobic digestion.* International journal of environmental research and public health, 2018. **15**(10): p. 2224.
31. Ma, J., et al., *A simple methodology for rate-limiting step determination for anaerobic digestion of complex substrates and effect of microbial community ratio.* Bioresource technology, 2013. **134**: p. 391-395.
32. Lin, L., et al., *In-depth investigation of enzymatic hydrolysis of biomass wastes based on three major components: cellulose, hemicellulose and lignin.* Bioresource technology, 2010. **101**(21): p. 8217-8223.
33. Akuzawa, M., et al., *Distinctive responses of metabolically active microbiota to acidification in a thermophilic anaerobic digester.* Microbial ecology, 2011. **61**: p. 595-605.
34. Stams, A.J. and C.M. Plugge, *Electron transfer in syntrophic communities of anaerobic bacteria and archaea.* Nature Reviews Microbiology, 2009. **7**(8): p. 568-577.
35. Ferry, J.G., *The chemical biology of methanogenesis.* Planetary and Space Science, 2010. **58**(14-15): p. 1775-1783.
36. Kiener, A. and T. Leisinger, *Oxygen sensitivity of methanogenic bacteria.* Systematic and Applied Microbiology, 1983. **4**(3): p. 305-312.
37. Mao, C., et al., *Review on research achievements of biogas from anaerobic digestion.* Renewable and sustainable energy reviews, 2015. **45**: p. 540-555.
38. Craggs, R., *Potential Energy Recovery by Anaerobic Digestion of Dairy Farm Waste.* NIWA: Hamilton, New Zealand, 2006.
39. Hartmann, H. and B.K. Ahring, *Strategies for the anaerobic digestion of the organic fraction of municipal solid waste: an overview.* Water science and technology, 2006. **53**(8): p. 7-22.
40. Kougias, P., K. Boe, and I. Angelidaki, *Effect of organic loading rate and feedstock composition on foaming in manure-based biogas reactors.* Bioresource technology, 2013. **144**: p. 1-7.
41. *Types of Anaerobic Digesters*. 25.02.2025]; Available from: https://www.epa.gov/anaerobic-digestion/types-anaerobic-digesters#:~:text=A%20wet%20digester%20or%20low,than%2015%20percent%20solids%20content.

 doi:10.20944/preprints202602.1296.v1

42. Bartholomew, C.H., *Mechanisms of catalyst deactivation.* Applied Catalysis A: General, 2001. **212**(1-2): p. 17-60.
43. Stewart, D. and B.B. Trangmar, *Methane from animal waste management systems*. 2008: Ministry of Agriculture and Forestry.
44. Severinsen, I., A. Herritsch, and M. Watson, *Modeling kinetic, thermodynamic, and operational effects in a steam methane reformer. Part A: reformer output.* Industrial & Engineering Chemistry Research, 2021. **60**(5): p. 2041-2049.
45. Dincer, I., *Comprehensive energy systems*. 2018: Elsevier.
46. Quirino, P., et al., *Impact of kinetic models in the prediction accuracy of an industrial steam methane reforming unit.* Computers & Chemical Engineering, 2021. **152**: p. 107379.
47. Young, A., et al., *Failure of commercial extruded catalysts in simple compression and bulk thermal cycling.* International Journal of Applied Ceramic Technology, 2018. **15**(1): p. 74-88.
48. Murkin, C. and J. Brightling, *Eighty years of steam reforming.* Johnson Matthey Technology Review, 2016. **60**(4): p. 263-269.
49. Chen, L., et al., *Catalytic hydrogen production from methane: A review on recent progress and prospect.* Catalysts, 2020. **10**(8): p. 858.
50. Vogt, C., et al., *Structure sensitivity in steam and dry methane reforming over nickel: activity and carbon formation.* ACS Catalysis, 2019. **10**(2): p. 1428-1438.
51. Jones, G., et al., *First principles calculations and experimental insight into methane steam reforming over transition metal catalysts.* Journal of Catalysis, 2008. **259**(1): p. 147-160.
52. Ganguli, A. and V. Bhatt, *Hydrogen production using advanced reactors by steam methane reforming: a review.* Frontiers in Thermal Engineering, 2023. **3**: p. 1143987.
53. Król, A., et al., *Hydrogen purification technologies in the context of its utilization.* Energies, 2024. **17**(15): p. 3794.
54. Lider, A., et al., *Materials and techniques for hydrogen separation from methane-containing gas mixtures.* International Journal of Hydrogen Energy, 2023. **48**(73): p. 28390-28411.
55. Angelidaki, I., et al., *Defining the biomethane potential (BMP) of solid organic wastes and energy crops: a proposed protocol for batch assays.* Water science and technology, 2009. **59**(5): p. 927-934.
56. Holliger, C., et al., *Towards a standardization of biomethane potential tests.* Water Science and Technology, 2016. **74**(11): p. 2515-2522.
57. Ohemeng-Ntiamoah, J. and T. Datta, *Perspectives on variabilities in biomethane potential test parameters and outcomes: A review of studies published between 2007 and 2018.* Science of the Total Environment, 2019. **664**: p. 1052-1062.
58. Buswell, A. and H. Mueller, *Mechanism of methane fermentation.* Industrial & Engineering Chemistry, 1952. **44**(3): p. 550-552.
59. Ragab, S.S., S.A. Khader, and E.K. Abd Elhamed, *Nutritional and chemical, studies on kiwi (Actinidia deliciosa) fruits.* J Home Econ, 2019. **29**(2): p. 4.
60. Onivogui, G., et al., *Chemical composition, nutritional properties and antioxidant activity of monkey apple (Anisophyllea laurina R. Br. ex Sabine).* Journal of Food and Nutrition Research, 2014. **2**(6): p. 281-287.
61. Sablani, S.S. and A.S. Mujumdar, *27 Drying of Potato, Sweet Potato, and Other Roots.* 2006.
62. Lao, L., et al., *CFD modeling and control of a steam methane reforming reactor.* Chemical Engineering Science, 2016. **148**: p. 78-92.
63. Schnaars, K., *What every operator should know about anaerobic digestion*, in *WE&T*. 2012.
64. Monson, K., et al., *Anaerobic Digestion of Biodegradable Municipal Wastes: A Review, The Sustainable Environment Research Centre, University of Glamorgan*. 2007, ISBN 978-1-84054-156-5.
65. Dhar, H., et al., *Effect of organic loading rate during anaerobic digestion of municipal solid waste.* Bioresource Technology, 2016. **217**: p. 56-61.
66. Kawai, M., et al., *The effect of the labile organic fraction in food waste and the substrate/inoculum ratio on anaerobic digestion for a reliable methane yield.* Bioresource technology, 2014. **157**: p. 174-180.
67. Hull-Cantillo, M., M. Lay, and P. Kovalsky, *Anaerobic Digestion of Dairy Effluent in New Zealand, Time to Revisit the Idea?* Energies, 2023. **16**(6): p. 2859.

 doi:10.20944/preprints202602.1296.v1

68. Gao, J., et al., *Mass conversion pathway during anaerobic digestion of wheat straw.* RSC advances, 2020. **10**(46): p. 27720-27727.
69. Pashchenko, D. and I. Makarov, *Carbon deposition in steam methane reforming over a Ni-based catalyst: Experimental and thermodynamic analysis.* Energy, 2021. **222**: p. 119993.